tagPAINT: Stoichiometric and covalent labelling of protein tags for multiplexed and quantitative DNA-PAINT imaging

Daniel J. Nieves[1,2], Geva Hilzenrat[1,2,3], Jason Tran[1,2], Zhengmin Yang[1], Hugh H. MacRae[1], Matthew A. B. Baker[4], J Justin Gooding[5] & Katharina Gaus[1,2*]

[1]EMBL Australia Node in Single Molecule Science, School of Medical Sciences, University of New South Wales, Sydney, Australia.

[2]ARC Centre of Excellence in Advanced Molecular Imaging, University of New South Wales, Sydney, Australia.

[3] Commonwealth Scientific and Industrial Research Organisation (CSIRO), Manufacturing, Clayton, VIC 3168, Australia.

[4]School of Biotechnology and Biomolecular Science, University of New South Wales, Sydney, NSW 2052, Australia.

[5]School of Chemistry, Australian Centre for NanoMedicine and the ARC Centre of Excellence in Convergent Bio-Nano Science and Technology, University of New South Wales, Sydney, Australia.

*Correspondence: k.gaus@unsw.edu.au

Abstract

We present a method for the stoichiometric labelling of expressed protein tags (SNAP tag and Halo tag) with single DNA docking strands, allowing the application of single molecule localisation microscopy via DNA-PAINT, termed tagPAINT. tagPAINT in then utilised for multiplexed and quantitative imaging of T-cell receptor signalling proteins.

Main Text

An important challenge for single molecule localization microscopy for quantitative measurements is control over the stoichiometry of the label to the molecule of interest. Lack of such control can confound or alter the observed biological behaviour and states of single molecules, complexes and structures due to suboptimal labelling[1, 2], crosslinking due to multivalency, or label-exchange[3]. To address these challenges approaches have been developed that allow a chemically versatile stoichiometric covalent linkage to be formed between biological molecule and fluorescent probes, in structurally defined positions[4, 5]. For example, stable and stoichiometric coupling of fluorescent labels to proteins of interest has been achieved through genetically encoded affinity tags[6, 7], non-canonical amino acid (ncAA) labelling[8, 9], and orthogonal chemistry[10, 11]. Such approaches have then been used to observe proteins at the single molecule level[10, 12].

Recently, Jungmann *et al.* demonstrated a SMLM approach using the binding/unbinding of short fluorescently conjugated DNA probes to antibodies labelled with complementary target strands, known as DNA PAINT[13-16]. This approach was extended to determine the number of proteins/targets present in sub-diffraction structures, termed qPAINT[17]. This method abrogates the uncertainty associated with the stochastic nature of fluorophore blinking and exploits *a priori* knowledge of the binding/unbinding behaviour of the probes. With this approach good agreement was achieved between the theoretical binding/unbinding rate and the observed number of proteins. However this approach relied on the use of probes labelled with multiple DNA target strands. Thus, multivalent interactions between proteins,and multiple target strands per protein, and incomplete labelling are still challenges that need to be addressed. More recently approaches to address this aim to minimise the linkage error, and include ncAA incorporation[8], affimers[18], and SOMAmers[19] which all allow 1:1 functionalization. However, although SOMAmers spend a long time bound, they still rely on a non-covalent interaction, and can potentially dissociate during long imaging times. Similarly, affimers are non-covalent, and sometimes require post-fixation, which may lead to off-target labelling. Also these reagents are only available for a few protein targets to date. Finally, while ncAA incorporation does allow a covalent stoichiometric linkage, it suffers from low expression and efficiency for labelling. New approaches which allow covalent and stoichiometric labelling of a protein of interest, while maintaining a low linkage error, would thus allow robust counting of protein numbers within cell, and thus full sampling of the heterogeneity therein[16].

At present there are a variety of methods to label proteins of interest covalently. One approach is incorporation of an enzymatically active tag, such as SNAP/CLIP-tag[20] and Halo Tag[21] technology. The Halo tag makes use of a chemical reaction orthogonal to eukaryotes, *i.e.*, the dehalogenation of haloalkane ligands, thus, leading to highly specific covalent labelling of the tag, and therefore protein[21], in both live and fixed cells. Haloalkanes can be modified to bear fluorescent labels, and has been demonstrated before for single molecule localisation microscopy (SMLM) in live cells using ATTO dye modified ligands[10]. Similarly, SNAP tag, a mutant of DNA repair protein O^6-alkylguanine-DNA alkyltransferase, can be covalently modified using O^6-benzylguanine substrates (BG), and has also been demonstrated to be suitable for SMLM imaging[22]. Combining such tagging

systems with DNA-PAINT imaging opens up the possibility for robust quantitative imaging of proteins within cells with certainty that the stoichiometry of ligand:tag is 1:1, and, simultaneously reducing the linkage error (size of tags c.a. < 5 nm).

Here, SNAP-tag and Halo Tag technologies are exploited to allow stoichiometric labelling of single proteins with a DNA PAINT target strand (*i.e.*, 1 protein: 1 target strand). Amine-bearing DNA target strands are modified by a one-step covalent conjugation reaction to bear either a O^6-benzylguanine or Halo ligand, thus generating SNAP and Halo PAINT substrates. The specificity of the approach is demonstrated by targeting α-tubulin. The multiplexing potential of tagPAINT is then applied to cells co-expressing Halo-tagged CD3ζ and SNAP-tagged LAT in Jurkat T-cells. Finally, the stoichiometric nature of this method is exploited to enable quantitative imaging, and thus counting, of single SNAP tag-labelled CD3ζ -chains of the T-cell receptor (TCR) at synapse of activated Jurkat T-cells.

First, to demonstrate the specificity of the approach we targeted SNAP and Halo tagged-α-tubulin (**Fig. 1**). Halo and SNAP tagged proteins bind covalently to their ligands, thus functionalisation of these ligands with single DNA target strands makes them amenable to DNA-PAINT imaging. To this end we used 5'-amine functionalised DNA target strands and reacted them either with excess of O^6-benzylguanine -NHS or Halo ligand-NHS ligands in a single step reaction (**Supplementary Scheme 1 and 2**). The product was then purified by size exclusion chromatography to remove the excess unreacted ligands, and used to label tag-expressing cells (**Fig. 1a and b**). NIH-3T3 cells, expressing both SNAP (**Fig. 1a**) and Halo-tagged (**Fig. 1b**) α-tubulin were labelled with the respective ligands and imaged using a complementary imaging strand labelled with Cy3B. It is clearly observed for both of the tags that the imager strand is directed to tubulin fibres. However, breaks in the fibre structure are observed (**Fig. 1a and b, i-iv**). This likely arises due to the fact that we express only one of the tubulin subunits, α-tubulin, and the presence of endogenous α-tubulin.

Having achieved specific targeting of the both SNAP and Halo-tagged proteins for DNA-PAINT in isolation, we sought to demonstrate the potential for multiplexed imaging with these two tags for DNA-PAINT. We used CD3ζ-knockout Jurkat T-cells and expressed both a Halo-tagged CD3ζ chain and SNAP-tagged LAT protein (**Fig. 2a**). These proteins are involved in the early signalling of T-cell activation and have been shown to associate and co-cluster upon engagement of the TCR[23]. Here, each protein was labelled with a ligand bearing different target sequences (P03 and P01), with SNAP-LAT being imaged with 2 nM of Cy3B labelled P03 imager and Halo-tagged CD3ζ imaged with 2nM ATTO655 conjugated P01 imager. DNA-PAINT signal is observed from both SNAP-LAT and Halo-CD3ζ proteins within the cell membrane (**Fig.2b, i-ii**). Thus, it is possible to orthogonally target and image different proteins within cells by employing the two tagging methods simultaneously.

Given that the stoichiometry of docking strand to protein target is 1:1, we used our approach to measure the stoichiometry of tagged CD3ζ within the membrane using quantitative DNA-PAINT (qPAINT). Quantitative tagPAINT data were acquired in CD3ζ-knockout Jurkat T-cells transfected with SNAP tag-labelled CD3ζ on activating antibody coated coverslips (**Fig 3a** and **3b**) using 5 nM ATTO655 imaging strand. Implementation of such analysis relies heavily on the ability to calibrate the association rate to obtain the characteristic dark time (τ_d), of the imager strand with the target strand[17]. Previously, Jungmann *et al*. employed DNA origami structures with target stands at specific positions on the origami to calibrate the association of DNA imaging strands with the target for a given experimental imager concentration[17]. By observing repeated binding events at these sites within the origami, it was then possible to measure the τ_d for a single target site, which was then used as a standard for calculating the number of sites within an unknown sample. Using a similar calibration method, within the same sample, we used a DNA origami block bearing a single target strand,

complementary to the imager strand, which were dispersed on the coverslip and anchored using avidin-biotin chemistry. It is evident from the images that single punctate features could be observed within the membrane of the cell (**Fig 3a**; zoomed regions **i-iv**). For quantitative analysis, the pointillistic tagPAINT data were automatically segmented using clustering algorithm (DBSCAN[24]), thus generating regions of interest for quantitative analysis. The points within the clusters were then used in conjunction with their time of appearance to calculate the characteristic dark time for that cluster, τ_d (**Fig.3b**). This was done for both the single site origami and the SNAP-tagged CD3ζ. The mean dark times for the single site origami calibration and the SNAP-tagged CD3ζ were 110.0 ± 4.1 s and 112.2 ± 4.2 s, respectively (mean ratio = 1.0 ± 0.1). Thus, population SNAP-tagged CD3ζ is largely monomeric, given its similarity to the dark time distribution for the single site calibration. CD3ζ chains are a dimer within the TCR-CD3 complex (**Fig. 3b**), however, when the chain is stretched out (approximately 35 nm in length, with the added diameter of the SNAP-tag) it is possible that the SNAP-tagged C-termini of a CD3ζ chains could lay far enough apart to be resolved, given that the linkage error of this approach is inherently smaller than conventional labelling. These data show that it is possible to detect individual SNAP-tagged proteins even though the overall distribution of receptor in activated T cells is non-random[25].

In conclusion, we demonstrate the covalent conjugation of DNA target strands to SNAP and Halo tag-labelled proteins stoichiometrically (1 protein: 1 DNA target), termed tag-PAINT. Firstly, we demonstrated the specificity of the approach by targeting tubulin in transfected cells. Further the potential for multiplexed imaging (both tags in the same cell) of CD3ζ and LAT in activated CD3ζ knockout Jurkat T-cells was achieved. Finally, exploiting the stoichiometry of conjugation we quantified the number of CD3ζ within the membrane of the same knockout Jurkat T-cells, and were able to observe largely single copies of the protein.

Main Figures

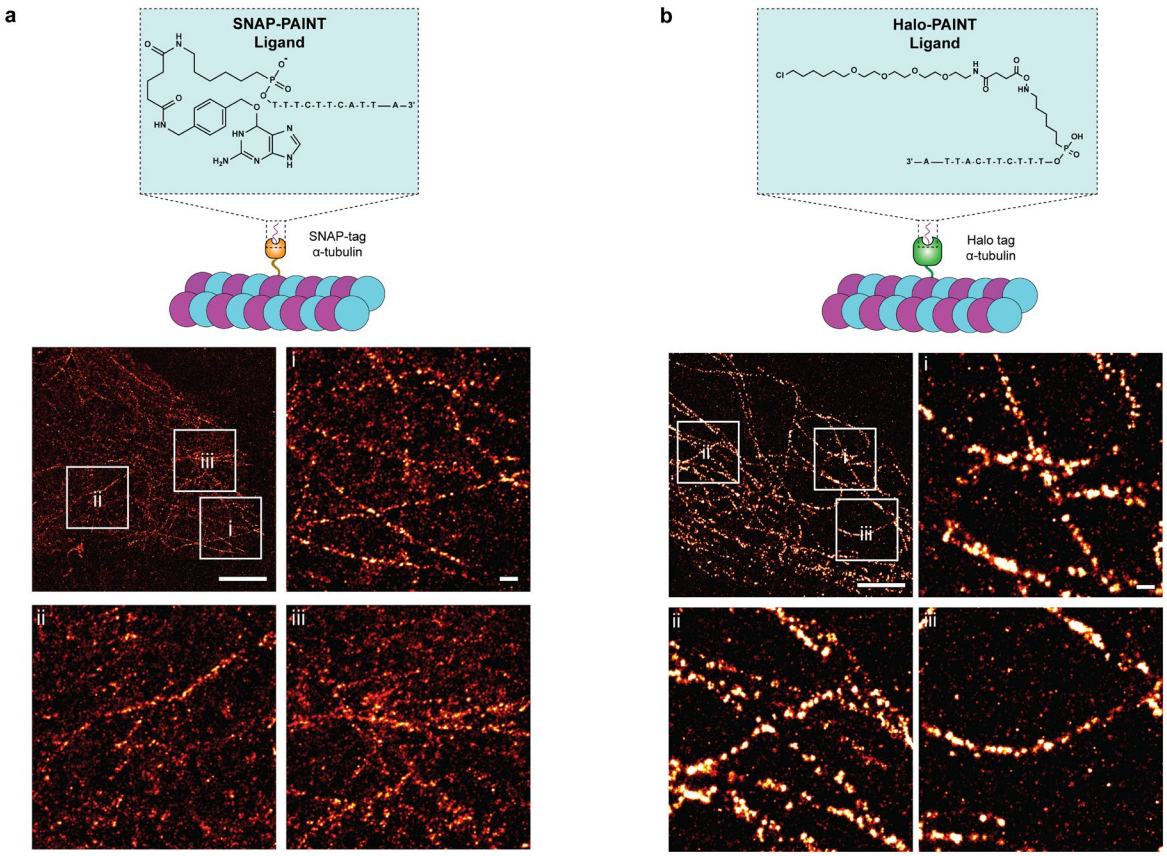

Fig. 1. Specific labelling and DNA-PAINT imaging of α-tubulin via tagPAINT. a. DNA-PAINT imaging of NIH-3T3 cell expressing SNAP-tagged α-tubulin (orange), labelled with SNAP-PAINT ligand (top, blue box). Images were acquired using Cy3B labelled imaging strand. **b**. DNA-PAINT imaging of NIH-3T3 cell expressing Halo tagged α-tubulin (green), labelled with Halo-PAINT ligand (top, blue box). Images were acquired using Cy3B labelled imaging strand at 2 nM. Scale bars are 5 μm (top left panels) and 50 nm zoomed regions (i-iii).

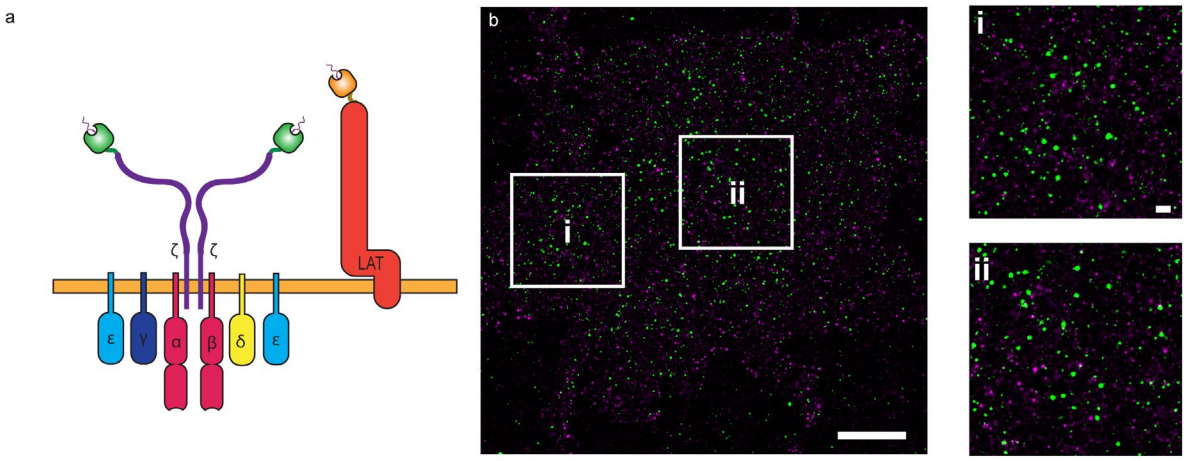

Fig. 2. Multiplexed tagPAINT imaging of CD3ζ and LAT in CD3ζ knockout Jurkat T-cells. a. CD3ζ knockout Jurkat T-cells were co-transfected with SNAP-tagged LAT and Halo tagged CD3ζ. Cells were labelled with both SNAP-PAINT (P03 docking strand) and Halo-PAINT (P01 docking strand) ligands. Cells were imaged sequentially with two different imaging strands, a Cy3B labelled imager (2 nM) directed to the SNAP-LAT and an ATTO655 imager (also 2 nM) for the Halo-CD3ζ. **b**. Overlayed tagPAINT images (left) of SNAP-LAT (magenta) and Halo-CD3ζ (green). Scale bars are 2 μM and 500 nm for zoomed images.

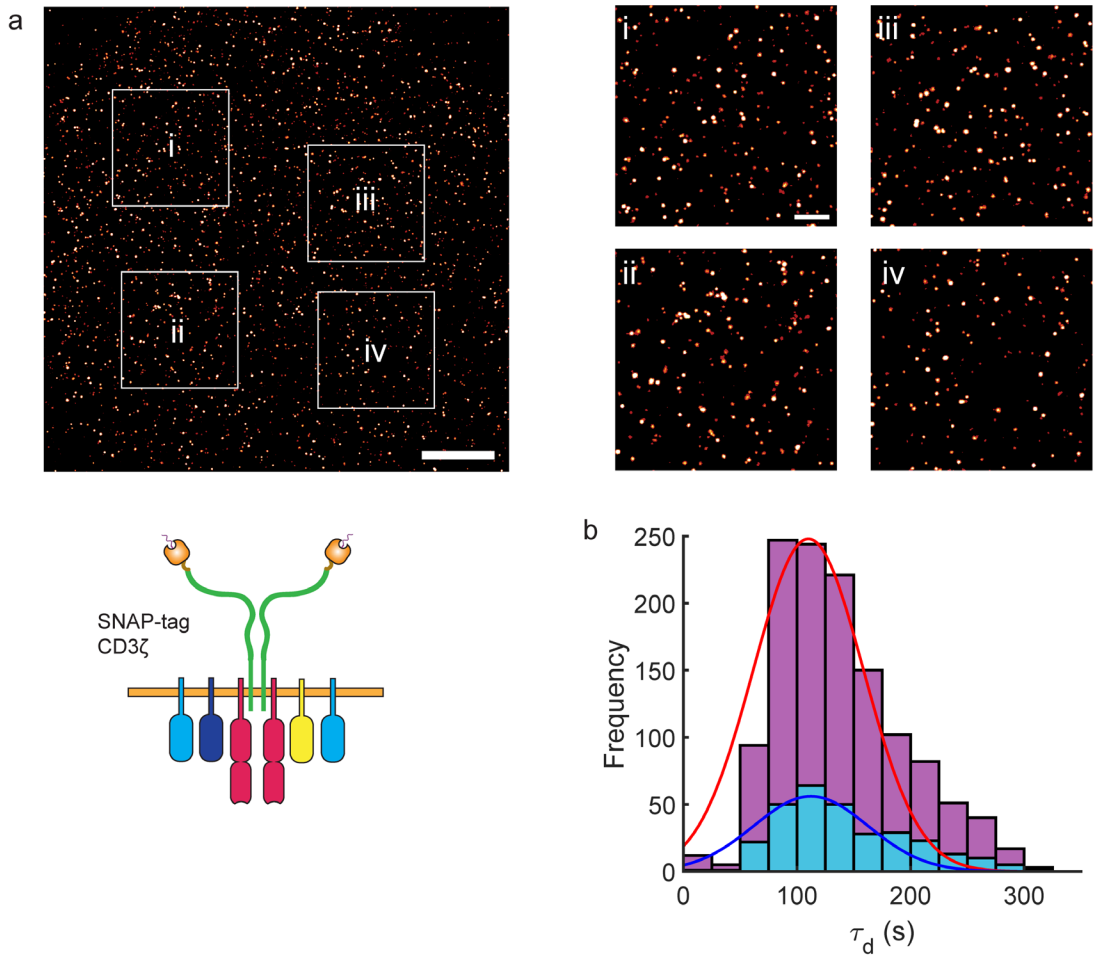

Fig. 3. Quantitative tagPAINT imaging of SNAP-CD3ζ. a. CD3ζ-knockout Jurkat T-cells were reconstituted with SNAP-tagged CD3ζ. Cells were labelled with SNAP-PAINT (P01 docking strand) and imaged with ATTO655 imager (5 nM). Scale bars 2 μM and 500 nm for zoomed images (**i-iv**). **b**. Dark-time distributions for single site origami calibration (purple) and SNAP-tagged CD3ζ (cyan). Both have been fit by a single Gaussian (origami calibration – red; SNAP-tagged CD3ζ - blue).

Online Methods and Materials

Plasmids. Tubulin-C-18 and were a gift from Michael Davidson (Addgene plasmid # 58197; http://n2t.net/addgene:58197 ; RRID:Addgene_58197). TUBB5-Halo was a gift from Yasushi Okada (Addgene plasmid # 64691; http://n2t.net/addgene:64691; RRID:Addgene_64691). For the expression of Halo Tag-labelled human CD3ζ, the EGFP gene in the vector pEGFP-N1 was exchanged with the Halo Tag gene after restriction digest, generating an empty back bone where human CD3ζ could be inserted. For SNAP-CD3ζ the Halo tag was subsequently replaced with SNAP gene, using the AgeI and NotI sites. For SNAP-LAT, human CD3ζ of the SNAP-CD3ζ construct was replaced with human LAT

Dye conjugated DNA imaging strands. P03Cy3B: 5'-GTAATGAAGA-Cy3B-3' (**Fig.1** and **Fig.2**, both at 2 nM), P01ATTO655: 5'- CTAGATGTAT-ATTO655-3' (**Fig.2**; 2nM, and **Fig.3**; 5nM).

Single site calibration DNA origami synthesis. A 115 helix DNA nano-cuboid was synthesised by annealing an m13mp19 genome back bone with 276 complementary staple strands (Supplementary Table 1). Four staple extensions (5'-TGCGCAACTTGTGAAGTGTC-3') that were complementary to 20 nt biotinylated DNA strands (5'-biotin/GACACTTCACAAGTTGCGCA-3') were incorporated on the bottom side of the cube to immobilise the nanotubes on streptavidin-coated surfaces. A further eleven 20 nucleotide staple extensions (5'-GTCACCATGTACCAATAGCG-3') were placed on the upper surface of the nano-cuboid to bind to complementary fluorescent oligos labelled with Alexa488 (5'-CGCTATTGGTACATGGTGAC-3'). Finally, the staple on helix 16 was extended to bear a single DNA-PAINT target sequence (P03; TTTCTTCATTA). The mixture was annealed for 24 hours (details) and subsequently gel purified for use.

Synthesis of Halo tag-DNA ligands. 5'amino modified DNA-docking strands were diluted in 10 mM sodium phosphate buffer pH 6.8, supplemented with 5 mM EDTA, to a final concentration of 1 mM. *N*-hydroxysuccinimidyl ester functionalised Halo tag ligand (NHS-HL) was freshly reconstituted in dry DMSO to a final concentration of 50 mM (unused NHS-HL was aliquoted and stored at -80°C). NHS-HL was diluted 10 times by adding 5'amino modified DNA-docking strands and mixing thoroughly. The reaction was left for 1 h at room temperature. The reaction product, HL functionalised with a DNA-docking strand was purified from excess unreacted NHS-HL by size exclusion chromatography, with 10 mM Tris supplemented with 1 mM EDTA as the mobile phase. Purified HL-DNA-docking strands were aliquoted and stored at -20°C until use (final concentration approximately 100-200 μM).

Synthesis of SNAP tag-DNA ligands. 5'amino modified DNA-docking strands were diluted in 10 mM sodium phosphate buffer pH 6.8, supplemented with 5 mM EDTA, to a final concentration of 1 mM. *N*-hydroxysuccinimidyl ester functionalised SNAP ligand (O^6-benzylguanine) was freshly reconstituted in dry DMSO to a final concentration of 50 mM (unused NHS- O^6-benzylguanine was aliquoted and stored at -80°C). NHS- O^6-benzylguanine was diluted 10 times by adding 5'amino modified DNA-docking strands and mixing thoroughly. The reaction was left for 1 hour at room temperature. The reaction product, O^6-benzylguanine functionalised with a DNA-docking strand was purified from excess unreacted NHS- O^6-benzylguanine by size exclusion chromatography, with 10 mM Tris supplemented with 1 mM EDTA as the mobile phase. Purified HL-DNA-docking strands were aliquoted and stored at -20°C until use (final concentration approximately 100-200 μM).

Transfection and fixation of NIH-3T3 cells. NIH-3T3 cells were transfected with Halo or SNAP constructs using Lipofectamine-3000 (ThermoFisher) following the manufacturers guidance. Briefly

cells were seeded to 50% confluency on clean glass coverslips. Cells in DMEM were incubated with a mix of 5 µg SNAP or Halo tagged alpha tubulin with Lipofectamine 300 and P300 reagent in Optimem for 24 h. Cells were then washed and pre-extracted using a microtubule stabilising buffer (BRB80+ 4mM EGTA) supplemented with Tween-20 0.5% (v/v) for 30 s and then fixed by adding an equal volume of 8% (v/v) PFA in microtubule stabilising buffer.

Transfection and fixation of Jurkat T-cells. E6.1 Jurkat T cells were transfected with Halo or SNAP constructs using an Invitrogen Neon Electroporation Transfection System (Life Technologies Pty Ltd.), using 3 pulses of 1350 V lasting 10 ms. The cells were left to recover after transfection in RPMI medium without Phenol Red (6040, GIBCO) supplemented 20 % (v/v) fetal bovine serum. Before seeding cells were pelleted by centrifugation, washed once with PBS and then resuspended in PBS. Cells we then used for seeding onto coverslips coated with 10 µg/mL anti-human CD3ε (activating) for 10 min at 37°C with 5% CO_2, after which non-adherent cells were washed away with PBS and then fixed with freshly prepared warm 4% (w/v) PFA in PBS for 10 mins. Fixative was then washed away with PBS and then cells were permeabilised for labelling with 0.1% (v/v) Triton X-100 in PBS for 3 min.

Labelling with SNAP and Halo DNA ligands. Both DNA-functionalised SNAP and Halo ligands were incubated with fixed cell samples at a final concentration of 5 µM in PBS supplemented with 0.2% Tween-20 (PBST) for 10 min. The samples were then vigorously washed with 1 mL of PBST, several times to remove any non-specifically adsorbed ligand. Finally, the samples were incubated with gold nanorods (Nanopartz) in PBST for 10 mins before mounting for tagPAINT imaging.

tagPAINT imaging. Prior to imaging labelled cells, glass coverslips were mounted into a chamlide chamber and freshly prepared imaging strands (**Fig. 1**: 1 nM Cy3B P03, **Fig. 2**: 2nM Cy3B P03, 2nM ATTO655 P01, **Fig. 3**: 5nM ATTO655 P01) in PBST supplemented with 500 mM NaCl were added to the chamber. For tagPAINT imaging, Cy3B and ATTO655 imager binding was acquired with the 561 nm (0.100 kW/cm^2) and 642 nm (0.075 kW/cm^2) laser lines, respectively. For standard tagPAINT imaging (**Fig. 1-2**) an integration time of 80 ms was used, with a TIRF angle of 66.90°, with 50,000-10,0000 frames acquired. For quantitative tagPAINT imaging (**Fig. 3**) the integration time 300 ms for 50,000 frames with a TIRF angle of 66.90°. Images were acquired either as 256x256 (**Fig. 1**) of 512x512 (**Fig. 2-3**) sized images with a pixel size of 97 nm.

tagPAINT processing and quantitative analysis. tagPAINT images were processed using Zeiss Zen Black software. The position of bound imaging strands in the acquisition was determined by Gaussian fitting, using a peak mask radius size of 6 pixels and a signal to noise ratio cut-off of 8. The localisation data was then drift corrected using the point patterns generated from the localisation of gold nanorod fiducials within the field of view using the Zeiss Zen Black software drift correction. The resulting localisation table was used for further analysis without modification. DBSCAN was used to group x,y localisation data of DNA imaging strands into clusters, with minPts = 20 and ε = 15 nm. Localisations assigned to clusters were then analysed for the frequency of events from binding/unbinding of detected DNA imaging strands. Firstly, time traces for events in each cluster over time were generated and the time between events, *i.e.*, the dark time, was extracted. The exponential CDF of the dark times was fitted to a single exponential, and the dark time corresponding to *1-1/e* extracted. For DNA origamis calibration samples, this number was used to deduce the dark time for a single site, τ_d. For the number of molecules per cluster from Halo-PAINT data characteristic dark time for a cluster, τ_d^C, was extracted and divided by τ_d.

Supplementary Information

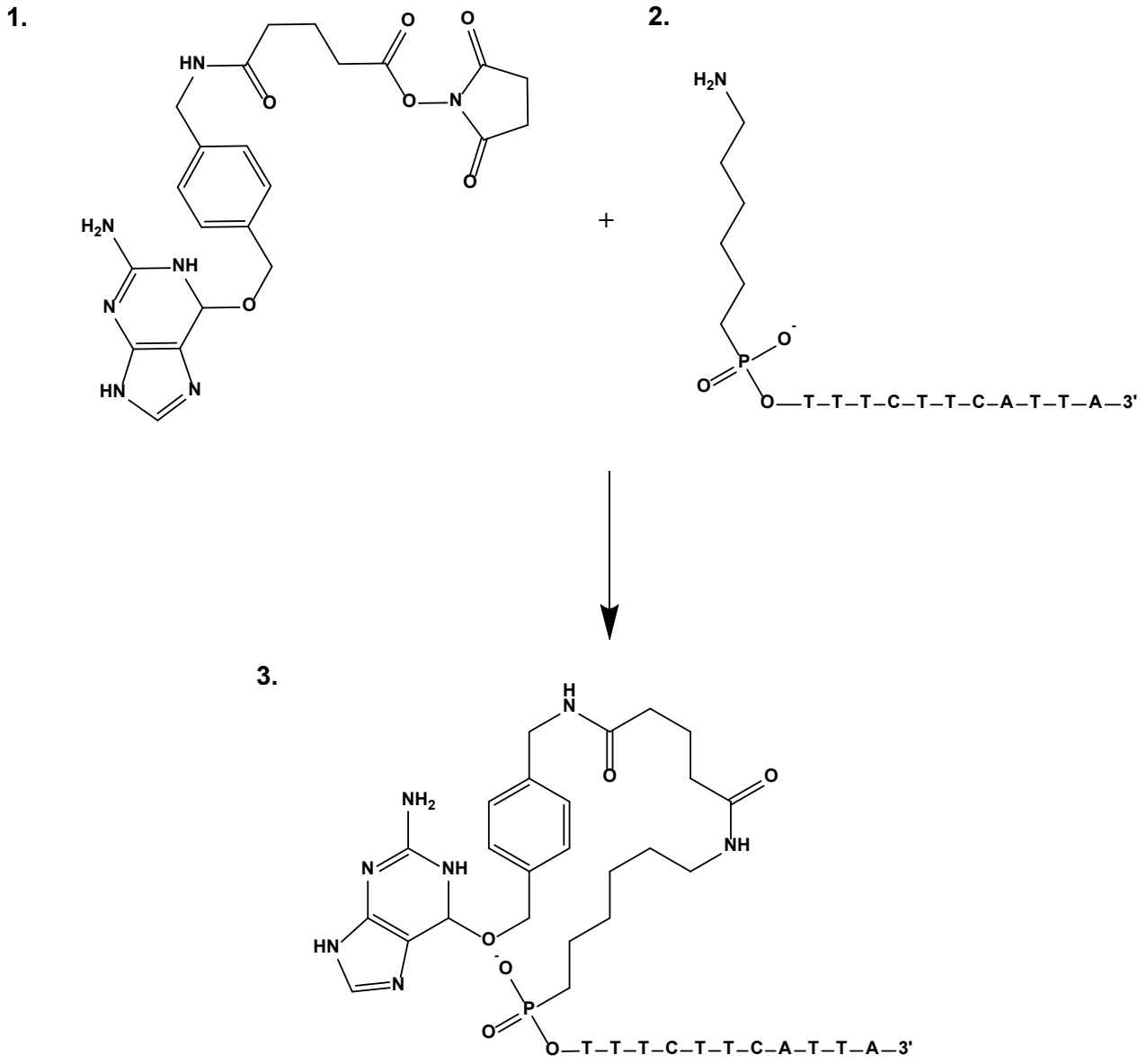

Supplementary Scheme 1. Synthesis of SNAP-PAINT ligand. *N*-hydroxysuccinimidyl ester functionalised SNAP ligand (NHS-O^6-benzylguanine, **1.**) was freshly reconstituted in dry DMSO to a final concentration of 50 mM (unused NHS-O^6-benzylguanine was aliquoted and stored at -80°C). 5'amino modified DNA-docking strands (**2.**) were diluted in 10 mM sodium phosphate buffer pH 6.8, supplemented with 5 mM EDTA, to a final concentration of 1 mM. . NHS-O^6-benzylguanine was diluted 10 times by adding 5'amino modified DNA-docking strands and mixing thoroughly (giving a 5:1 ratio of NHS-O^6-benzylguanine:5'amino DNA). The reaction was left for 1 hour at room temperature. The reaction product (**3.**), BG functionalised with a DNA-docking strand was purified from excess unreacted NHS-O^6-benzylguanine by size exclusion chromatography, with 10 mM Tris supplemented with 1 mM EDTA as the mobile phase. Purified HL-DNA-docking strands were aliquoted and stored at -20°C until use (final concentration approximately 100-200 µM).

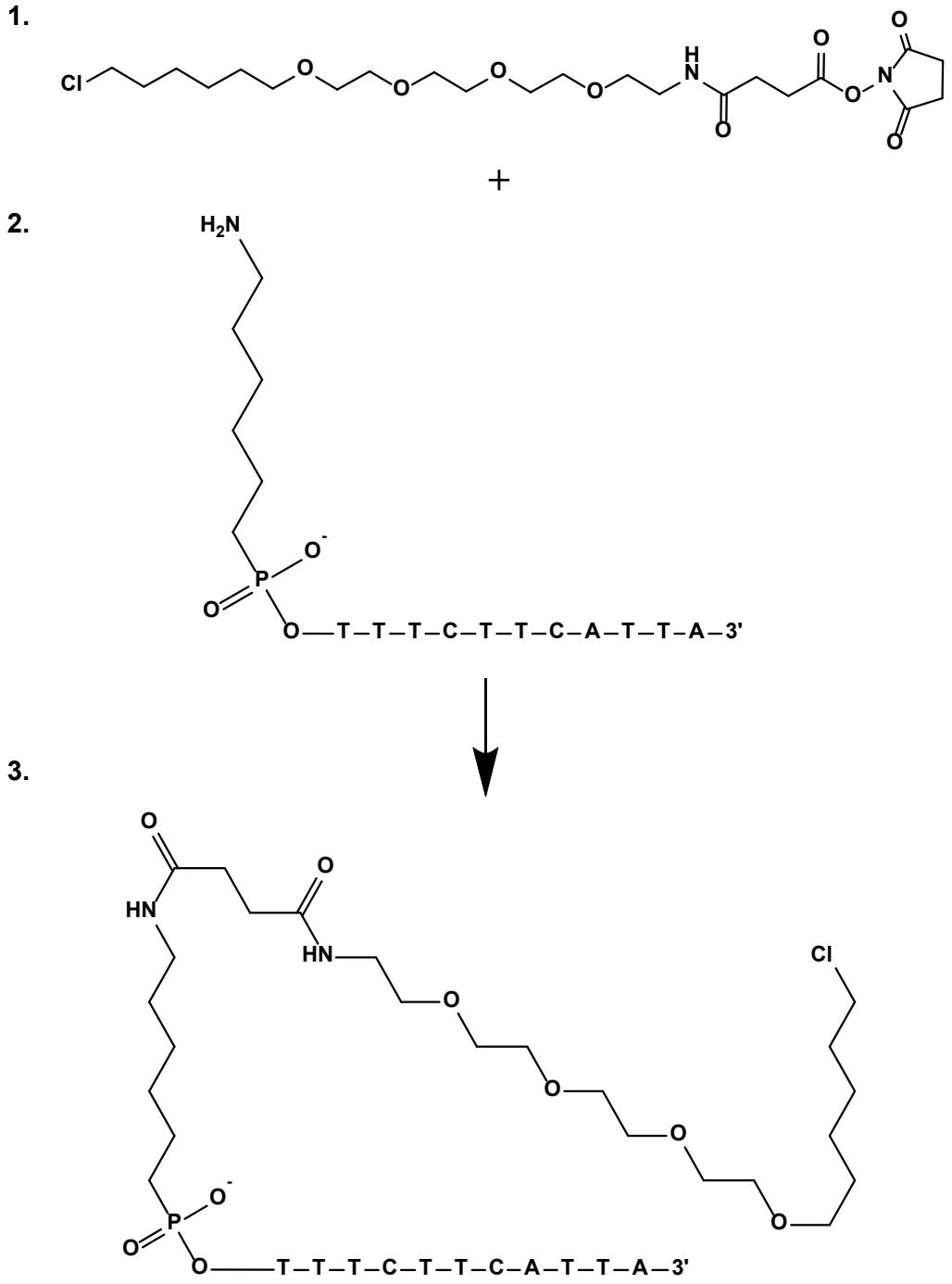

Supplementary Scheme 2. Synthesis of Halo-PAINT ligand. *N*-hydroxysuccinimidyl ester functionalised Halo tag ligand (NHS-HL, **1.**) was freshly reconstituted in dry DMSO to a final concentration of 50 mM (unused NHS-HL was aliquoted and stored at -80°C). 5'amino modified DNA-docking strands (**2.**) were diluted in 10 mM sodium phosphate buffer pH 6.8, supplemented with 5 mM EDTA, to a final concentration of 1 mM. . NHS-HL was diluted 10 times by adding 5'amino modified DNA-docking strands and mixing thoroughly (giving a 5:1 ratio of NHS-HL:5'amino DNA). The reaction was left for 1 h at room temperature. The reaction product (**3.**), HL functionalised with a DNA-docking strand was purified from excess unreacted NHS-HL by size exclusion chromatography, with 10 mM Tris supplemented with 1 mM EDTA as the mobile phase. Purified HL-DNA-docking strands were aliquoted and stored at -20°C until use (final concentration approximately 100-200 µM).

References

1. Ehmann, N. et al. Quantitative super-resolution imaging of Bruchpilot distinguishes active zone states. *Nat Commun* **5**, 4650 (2014).
2. Whelan, D.R. & Bell, T.D. Image artifacts in single molecule localization microscopy: why optimization of sample preparation protocols matters. *Sci Rep* **5**, 7924 (2015).
3. Heinze, K.G., Costantino, S., De Koninck, P. & Wiseman, P.W. Beyond photobleaching, laser illumination unbinds fluorescent proteins. *J Phys Chem B* **113**, 5225-5233 (2009).
4. Baskin, J.M. et al. Copper-free click chemistry for dynamic in vivo imaging. *Proc Natl Acad Sci U S A* **104**, 16793-16797 (2007).
5. Saxon, E. & Bertozzi, C.R. Cell surface engineering by a modified Staudinger reaction. *Science* **287**, 2007-2010 (2000).
6. Barlag, B. et al. Single molecule super-resolution imaging of proteins in living Salmonella enterica using self-labelling enzymes. *Sci Rep* **6**, 31601 (2016).
7. Hauke, S., von Appen, A., Quidwai, T., Ries, J. & Wombacher, R. Specific protein labeling with caged fluorophores for dual-color imaging and super-resolution microscopy in living cells. *Chem Sci* **8**, 559-566 (2017).
8. Nikic, I. et al. Debugging Eukaryotic Genetic Code Expansion for Site-Specific Click-PAINT Super-Resolution Microscopy. *Angew Chem Int Ed Engl* **55**, 16172-16176 (2016).
9. Nikic-Spiegel, I. Genetic Code Expansion- and Click Chemistry-Based Site-Specific Protein Labeling for Intracellular DNA-PAINT Imaging. *Methods Mol Biol* **1728**, 279-295 (2018).
10. Wilmes, S. et al. Triple-color super-resolution imaging of live cells: resolving submicroscopic receptor organization in the plasma membrane. *Angew Chem Int Ed Engl* **51**, 4868-4871 (2012).
11. Tyagi, S. & Lemke, E.A. Genetically encoded click chemistry for single-molecule FRET of proteins. *Methods Cell Biol* **113**, 169-187 (2013).
12. Bosch, P.J. et al. Evaluation of fluorophores to label SNAP-tag fused proteins for multicolor single-molecule tracking microscopy in live cells. *Biophys J* **107**, 803-814 (2014).
13. Agasti, S.S. et al. DNA-barcoded labeling probes for highly multiplexed Exchange-PAINT imaging. *Chem Sci* **8**, 3080-3091 (2017).
14. Jungmann, R. et al. Multiplexed 3D cellular super-resolution imaging with DNA-PAINT and Exchange-PAINT. *Nat Methods* **11**, 313-318 (2014).
15. Schnitzbauer, J., Strauss, M.T., Schlichthaerle, T., Schueder, F. & Jungmann, R. Super-resolution microscopy with DNA-PAINT. *Nat Protoc* **12**, 1198-1228 (2017).
16. Nieves, D.J., Gaus, K. & Baker, M.A.B. DNA-Based Super-Resolution Microscopy: DNA-PAINT. *Genes (Basel)* **9** (2018).
17. Jungmann, R. et al. Quantitative super-resolution imaging with qPAINT. *Nat Methods* **13**, 439-442 (2016).
18. Schlichthaerle, T. et al. Site-Specific Labeling of Affimers for DNA-PAINT Microscopy. *Angew Chem Int Ed Engl* (2018).
19. Strauss, S. et al. Modified aptamers enable quantitative sub-10-nm cellular DNA-PAINT imaging. *Nat Methods* **15**, 685-688 (2018).
20. Gautier, A. et al. An engineered protein tag for multiprotein labeling in living cells. *Chem Biol* **15**, 128-136 (2008).
21. Los, G.V. et al. HaloTag: a novel protein labeling technology for cell imaging and protein analysis. *ACS Chem Biol* **3**, 373-382 (2008).
22. Klein, T. et al. Live-cell dSTORM with SNAP-tag fusion proteins. *Nat Methods* **8**, 7-9 (2011).
23. Lillemeier, B.F. et al. TCR and Lat are expressed on separate protein islands on T cell membranes and concatenate during activation. *Nature immunology* **11**, 90-96 (2010).
24. Ester, M.K., H.P.; Sander, J.; Xu X. A density-based algorithm for discovering clusters in large spatial databases with noise. *KDD-96 Proceedings* (1996).

25. Pageon, S.V. et al. Functional role of T-cell receptor nanoclusters in signal initiation and antigen discrimination. *Proc Natl Acad Sci U S A* **113**, E5454-5463 (2016).